

Evaluating Zn-Porphyrin-Based Near-IR-Sensitive Non-Fullerene Acceptors for Efficient Panchromatic Organic Solar Cells

Muhammad Usman Khan,^[a, b] Muhammad Imran,^[c, d] Muhammad Fayyaz ur Rehman,^[e] Mohammed A. Assiri,^[c, d] Syed Muddassir Ali Mashhadi,^[f] Muhammad Safwan Akram,^{*[g, h]} and Changrui Lu^{*[a]}

Porphyrin-based non-fullerene acceptors (NFAs) have shown pronounced potential for assembling low-bandgap materials with near-infrared (NIR) characteristics. Herein, **panchromatic-type porphyrin-based** molecules (POR1–POR5) are proposed by modulating end-capped acceptors of a highly efficient porphyrin-based NFA PORTFIC(POR) for organic solar cells (OSCs). Quantum chemical structure-property relationship has been studied to discover photovoltaic and optoelectronic characteristics of POR1–POR5. Results show that optoelectronic properties of the POR1–POR5 are better in all aspects when compared with the reference POR. All proposed NFAs particularly POR5

proved to be the preferable porphyrin-based NIR sensitive NFA for OSCs applications owing to lower energy gap (1.56 eV), transition energy (1.11 eV), binding energy ($E_b = 0.986$ eV), electron mobility ($\lambda_e = 0.007013E_h$), hole mobility ($\lambda_h = 0.004686 E_h$), high $\lambda_{max} = 1116.27$ nm and open-circuit voltage ($V_{oc} = 1.96$ V) values in contrast to the reference POR and other proposed NFAs. This quantum chemical insight provides sufficient evidence about excellent potential of the proposed porphyrin-based NIR sensitive NFA derivatives for their use in OSCs.

Introduction

The annual energy requirement of the world can easily be met with abundant solar energy that sun provides in just one hour.^[1] From one estimate, current energy consumption from world's fossil fuel resources is equal to what sun can provide in mere 1.5 days.^[2] Through photosynthesis, nature is getting advantage of solar energy^[3] by using an organometallic pigment chlorophyll which plays a vital role in capturing solar energy. Chlorophyll has a porphyrin ring, which is an archetypal planar heterocyclic chemical, with a metal in the centre.^[4]

Porphyryns are organic dyes that exhibit distinctive optoelectronic properties because of their eighteen delocalized π -electrons. They possess high molar absorption coefficients and remarkable light-harvesting capability, making them an ideal candidate for incorporation into modern organic solar devices.^[5] The porphyrin absorption range lies around 400–450 nm in the solet (blue) band while at 500–650 nm in Q (red) band region of visible spectrum. These ranges can be simply extended to near-infrared (NIR) region via use of acceptor-donor-acceptor (A-D-A) configuration that contains porphyrin as a donor core in the center.^[6] There are several efficient ways to tune the

[a] Dr. M. U. Khan, Dr. C. Lu
Department of Chemistry
Chemical Engineering and Biotechnology
Donghua University
Shanghai 201620 (P.R. China)
E-mail: crlu@dhu.edu.cn

[b] Dr. M. U. Khan
Department of Chemistry
University of Okara
Okara 56300 (Pakistan)

[c] Dr. M. Imran., Dr. M. A. Assiri
Research Center for Advanced Materials
King Khalid University
P.O. Box 9004
Abha 61514 (Saudi Arabia)


[d] Dr. M. Imran., Dr. M. A. Assiri
Department of Chemistry
Faculty of Science
King Khalid University
P.O. Box 9004
Abha 61413 (Saudi Arabia)


[e] Dr. M. F. u. Rehman
Department of Chemistry
University of Sargodha
Sargodha, 40100 (Pakistan)

[f] Dr. S. M. A. Mashhadi
Research University of Sialkot
Sialkot, 51040 (Pakistan)

[g] Dr. M. S. Akram
School of Health and Life Sciences
Teesside University
Middlesbrough TS1 3BA (UK)
E-mail: Safwan.akram@tees.ac.uk

[h] Dr. M. S. Akram
National Horizons Centre
Teesside University
Darlington, DL1 1HG (UK)

 Supporting information for this article is available on the WWW under <https://doi.org/10.1002/open.202200047>

 © 2022 The Authors. Published by Wiley-VCH GmbH. This is an open access article under the terms of the Creative Commons Attribution Non-Commercial License, which permits use, distribution and reproduction in any medium, provided the original work is properly cited and is not used for commercial purposes.

molecular characteristics such as extending the π -conjugated backbone length, changing the end-capped moieties or inserting different metal atoms into the porphyrin backbone.^[7] Although significant efforts have been made in synthesizing the main chain porphyrin polymer, but optoelectronic performance of porphyrin polymer still lags behind that of other conjugated polymer systems because of low charge transfer rate and unfavorable morphology.^[8]

The first example of interpolating dangling side chain of porphyrin into backbone of polymer has been reported by Chao et al.^[9] with a remarkable power conversion efficiency (PCE) of 8.6% due to enhancement of light harvesting ability of the polymer. Moreover, Peng group synthesized A-D-A configured a set of porphyrin core donor compounds in which rhodamine and diketopyrrolopyrrole electron withdrawing units were attached to both sides of the central core. Organic solar cells (OSCs) based on the fabrication of these porphyrin derivatives with PC₆₁BM or PC₇₁BM acceptor provided over 8% PCE.^[10] The development of porphyrin-based acceptors have gained increasing consideration over the years,^[11] where several efforts have been made on re-designing dyes with better electron withdrawing units which resulted better harvesting of light. For instance, Li et al. synthesized four new porphyrin molecules PBI-Por by incorporating perylene diimide (PDIs) units into porphyrin ring via Sonogashira coupling to obtain a wring type assembly. A noticeable PCE of 7.4% was achieved by blended PBI-Por with PBDB-T donor but it still suffered from insufficient light harvesting beyond 700 nm.^[12]

Electron deficient units termed as 2-(3-oxo-2,3-dihydroinden-1-ylidene)-malononitrile (IC) and 2-(5,6-difluoro-3-oxo-2, 3-dihydro-1H-inden-1-ylidene)-malononitrile (FIC) have shown promise or tailoring A-D-A type NFAs with un-fused or ladder type backbones.^[13] It was noticed that the introduction of IC and FIC unit not only maintains the molecular planarity of backbone but also is responsible for efficient intermolecular charge transfer (ICT) leading to red-shifted absorption.^[14] Lately, various acceptors containing ladder like backbone with IC and FIC end-capped moieties have been investigated and their results indicate that such acceptor molecules can stack to one another through FIC and IC unit.^[15] Lin et al. designed three porphyrin cored acceptors by linking thiophene-FIC group at meso position through a single bond in 2019.^[16] But these non-fullerene acceptors (NFAs) lack absorption above 600 nm due to free rotation of the single bonds that decreases the transfer of energy across the FIC and the porphyrin group.

In order to obtain panchromatic absorption, Wang et al.^[17] purposed a strategy of introducing ethynyl linkage to build new A-D-A types porphyrin core molecules. The ethynyl linker was correctly anticipated to improve the molecular planarity effectively extending the absorption spectra to harvest sunlight to NIR region. Therefore, two panchromatic porphyrin derivatives PORTIC and fluorinated PORTFIC were synthesized,^[17] with porphyrin as a central core, thiophene and ethynyl linkage as a bridge and IC, FIC end-capped acceptor units respectively. The effect on various electron-pulling units (H, F) on their analogous optoelectronic properties were investigated by Wang et al.^[17] The changing of H in PORTIC with F in PORTFIC significantly

affected the photovoltaic properties. Therefore, taking clue from this substitution, we planned to further substitute the end-capped acceptor of PORTFIC with various reported electron-pulling end-capped groups and develop new porphyrin-based near-infrared (IR) sensitive NFAs with better photovoltaic efficiency. Quantum chemical calculations using density functional theory (DFT) and time dependent DFT (TDDFT) have been performed to compute the optoelectronic properties of newly developed and reference molecule. The developed molecules with better photovoltaic characteristics have been recommended for constructing high-performance porphyrin-based near-IR sensitive NFAs.

Computational procedure

Calculations in current investigation are executed employing Gaussian 09 W^[18] and GaussView 5.0 program.^[19] Six widely reported and opted functionals for optoelectronic features estimation^[20] were tested to find the most suitable one for entire quantum chemical calculations of current study. The range of functionals include the global hybrid GGA method B3LYP, range-separated corrected methods ω B97XD, CAM-B3LYP, LC-BLYP, meta-hybrid GGA method M062X and hybrid functional MPW1PW91. Therefore, reference molecule PORTFIC's^[17] (POR) optimization was firstly done using B3LYP,^[21] ω B97XD,^[22] MPW1PW91,^[23] LC-BLYP,^[24] CAM-B3LYP,^[25] and M06-2X^[26] functionals. For H, C, N, S, O and F, 6-31G(d,p) basis set was adopted. Whereas, SDD (Stuttgart/Dresden double- ζ) and LANL2DZ basis sets were adopted for metal atom (Zn). At same DFT-functionals/6-31G(d,p)/SDD and DFT-functionals/6-31G(d,p)/LANL2DZ combinations, stability of the optimized geometries was confirmed because of the absence of imaginary frequency. The absorption maximum of POR was computed using TDDFT calculations on above mentioned levels of theory and basis set combinations. The twenty lowest singlet-singlet excitation energies were estimated from TDDFT computations. The solvent effect was computed using the conductor-like polarizable continuum model (CPCM).^[27] The good harmony of DFT computed absorption maxima with experimental λ_{max} of PORTFIC^[17] is detected with CAM-B3LYP/6-31G(d,p)/LANL2DZ combination. Consequently, it was selected for estimating the optoelectronic features of reference (POR) and the developed (POR1–POR5) molecules. Frontier molecular orbital (FMO) analysis, density of state (DOS), overlap density of state (ODOS) analysis, optical characteristics, open circuit voltage (V_{oc}), transition density matrix (TDM) and charge transfer analysis were performed using CAM-B3LYP/6-31G(d,p)/LANL2DZ combination. Similarly, photophysical features of POR1–POR5 molecules were predicted by estimating the lowest 20 excited states employing TDDFT/CAM-B3LYP/6-31G(d,p)/LANL2DZ combination.

Charge mobilities mainly rely on reorganization energy. The λ_{int} deals with swift internal environmental changes while, λ_{ext} represents external environmental transformations of various kinds and can be ignored due to its negligible role in this context. In this study, we only deal with λ_{int} which depends on

hole (λ_h) and electron (λ_e) reorganization energies, which are calculated using equations 1 and 2.^[28]

$$\lambda_e = [E_0^- - E_-] + [E_+^0 - E_0] \quad (1)$$

$$\lambda_h = [E_0^+ - E_+] + [E_+^0 - E_0] \quad (2)$$

Where E_+^0 and E_-^0 are the anionic and cationic optimized geometries energy values in neutral state. The superscript 0 in E_+^0 and E_-^0 represents neutral state. E_0 is single point energy at ground state. E_0^+ and E_0^- represent energy of neutral molecule in cation and anion states correspondingly. The E_- and E_+ are the energy value that of optimized anions and cations separately.^[29]

The PyMolyze 2.0,^[30] Origin 8.0, Avogadro,^[31] Chemcraft,^[32] and Multiwfn 3.7 program^[33] were employed for elucidating the data from output files.

Results and discussion

An effective molecular designing strategy for NFAs is to increase the intramolecular charge transfer and abridging the energy gap.^[34] Visible light accounts for less than 50% of the solar energy, while the rest is largely in the form infrared radiation which is not captured by the modern solar cells. This study aims to expand the photovoltaic and optoelectronic properties of porphyrin-based NIR sensitive NFAs via modification of end-capped acceptor units. For this, a newly synthesized porphyrin-

based NFA PORTFIC^[17] is modified (Figure 1) to design better photovoltaic precursors using (5,6-difluoro-2-methylene-3-oxo-2,3-dihydro-1H-inden-1-ylidene)methanesulfonic acid (P1), 3-(dinitromethylene)-5,6-difluoro-2-methylene-2,3-dihydro-1H-inden-1-one (P2), 2-(5,6-dichloro-2-methylene-3-oxo-2,3-dihydro-1H-inden-1-ylidene)malononitrile (P3), 1-(dicyanomethylene)-2-methylene-3-oxo-2,3-dihydro-1H-indene-5,6-dicarbonitrile (P4) and methyl 6-cyano-1-(dicyanomethylene)-2-methylene-3-oxo-2,3-dihydro-1H-indene-5-carboxylate (P5) end-capped groups present in POR1, POR2, POR3, POR4 and POR5 molecules, respectively (Figure 1).

In all developed NFAs, central core porphyrin along with above and below mentioned units act as a donor unit. 2-ethynyl-5-methylthiophene plays the role of the bridge unit. The difference between end-capped acceptors P1 and P2 is the presence of two SO₃H in P1 and two NO₂ groups in P2. The P3 end-capped acceptor contains two Cl and two CN groups. The end-capped acceptor P4 and P5 is having a difference of CN and COOCH₃ groups respectively. These all units along with their extended conjugation work collectively to generate successful ICT among molecules which leads to enhancement in optoelectronic characteristics of the investigated NFAs. The reference POR and developed POR1–POR5 molecules structures are shown in Figure 2. The λ_{max} of reference molecule at number of DFT functionals and basis set combinations are tested for opting the finest functional and results are portrayed in Figure 3.

The experimentally reported λ_{max} value of reference POR molecule is 810 nm.^[17] In combination with all levels of theory,

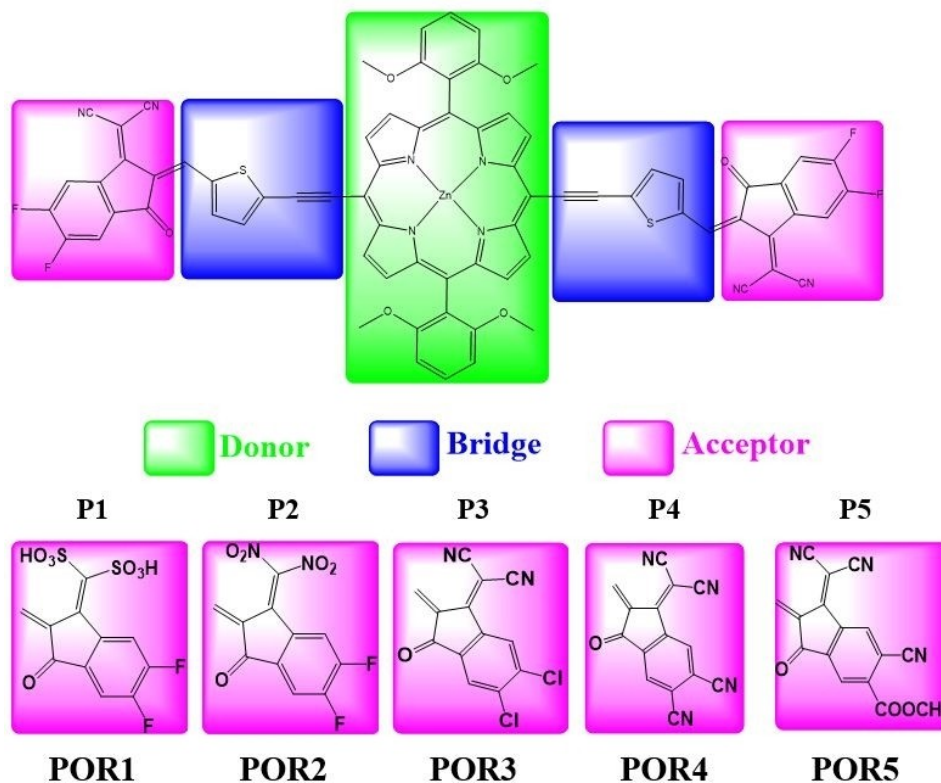


Figure 1. Sketch map of new porphyrin-based NIR sensitive NFAs.

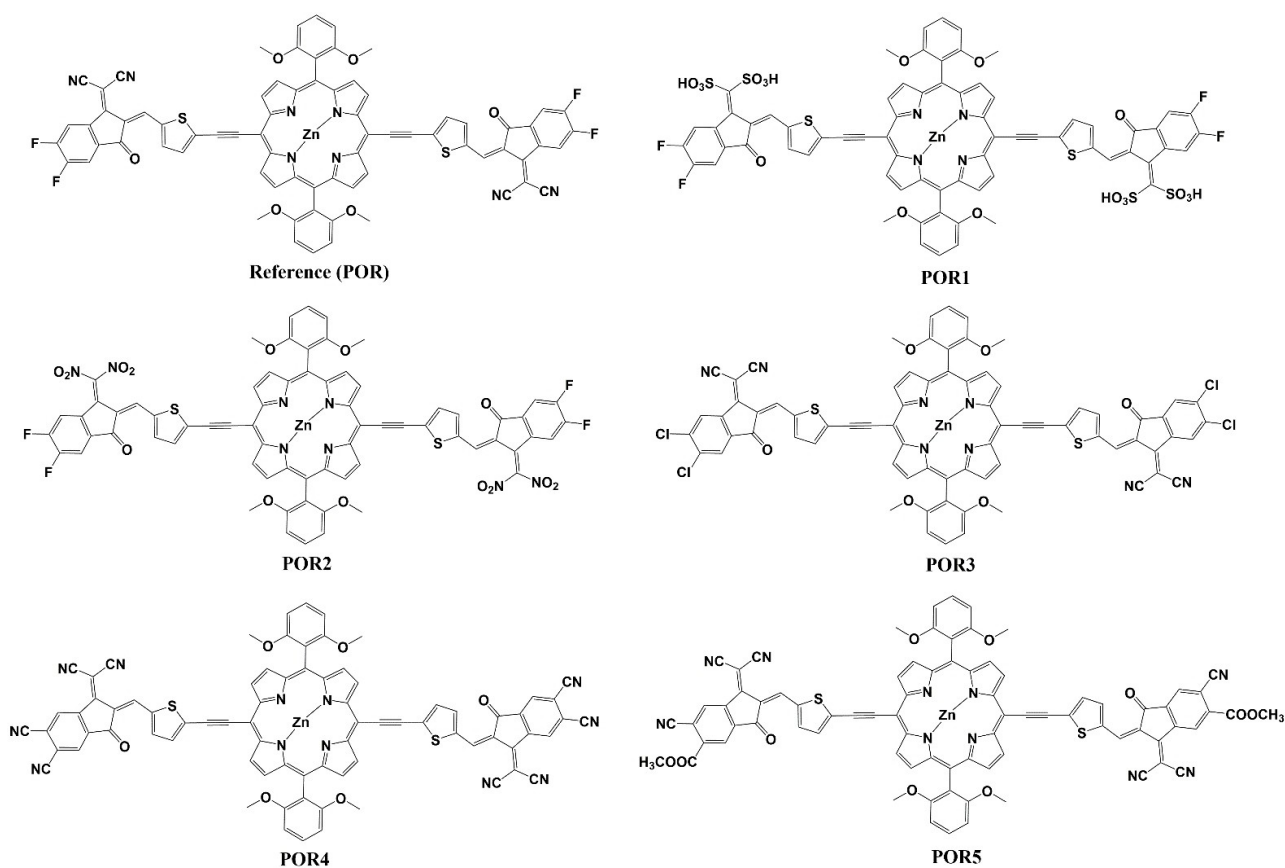


Figure 2. Molecular structures of reference POR and designed molecules POR1–POR5.

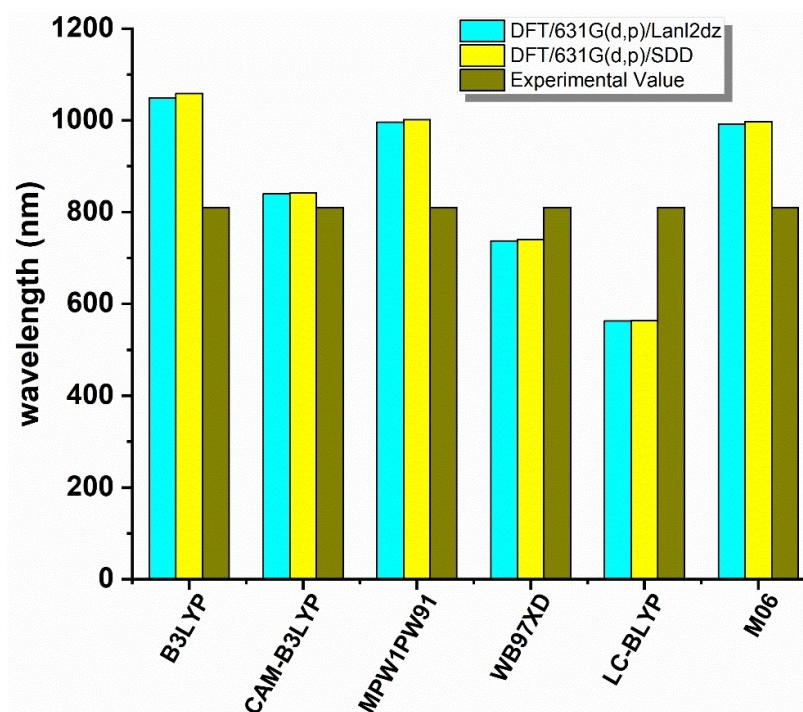


Figure 3. Bar chart of λ_{max} value for POR (reference) at different functionals and basis set combinations.

LANL2DZ exhibit closure to experimental λ_{max} values as compared to SDD basis set. Overall, Figure 3 indicates that CAM-B3LYP/6-31G(d,p)/LANL2DZ combination shows 840 nm λ_{max} value which is the best agreement with experimental λ_{max} value among all absorption maximum values computed from different functionals. Therefore, CAM-B3LYP/6-31G(d,p)/LANL2DZ is nominated for estimating the optoelectronic characteristics of reference (POR) as well as designed compounds (POR1–POR5).

Geometrical analysis

The geometry optimization of designed compounds (POR1–POR5) are accomplished at CAM-B3LYP/6-31G(d,p)/LANL2DZ functional and output geometries POR1–POR5 are presented in Figure 4. It is manifesting from the optimized geometries of POR and POR1–POR5 that central core porphyrin, bridge and few parts of end-capped units are grouped themselves in one plane. However, to limit the potential energy surface, OCH₃ substituted benzyl group on Zn-porphyrin and few parts of end-capped acceptor arrayed themselves out of the plane. The effect of end-cap group modifications on structural parameters is examined by computed bond lengths d_1 and d_2 and angles θ_1 and θ_2 . A generalized scheme that represents the d_1 , d_2 and θ_1 , θ_2 of studied NFAs is shown in Figure S1 (Supplementary

Information). The bond lengths d_1 and d_2 connect the thiophene bridge with end-capped acceptor units P1, P2, P3, P4, P5 along left and right sides of central core porphyrin respectively. Similarly, θ_1 and θ_2 is the dihedral angle present between bridge and end-capped acceptor motifs of studied molecules. The optoelectronic features are notable impacted by geometrical parameters of molecules. The calculated results of d_1 , d_2 and θ_1 , θ_2 are collected in Table S1 (Supplementary Information).

Results indicate that the d_1 and d_2 bond lengths in reference POR is found almost same 1.4344 and 1.4343 Å respectively. The effect of end-capped modifications shortens the bond lengths d_1 and d_2 in proposed molecules POR1–POR5 that lie the span of 1.4313–1.4342 and 1.4314–1.4342 Å respectively. Similarly, bond angles θ_1 and θ_2 are found close to each other. Minute difference in bond angles of POR and POR1–POR5 might due to attachment of thiophene with less sterically restricted end-capped unit that rotate freely.

Frontier molecular orbital analysis

The photovoltaic efficiency of OSC materials relies on the positions of HOMO, LUMO and the energy difference between the molecular orbitals.^[35] Photovoltaic performances of the materials are upgraded through shortening of the energy gap

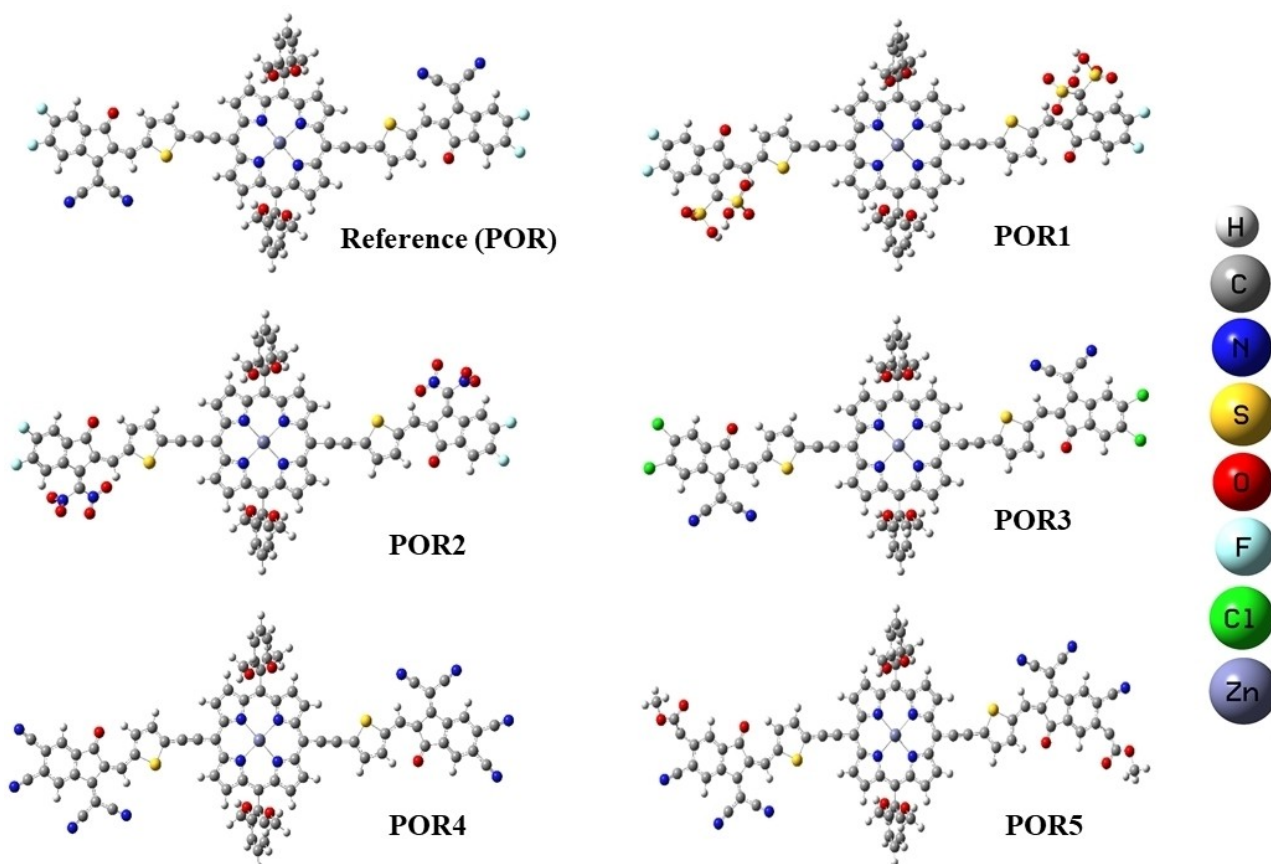


Figure 4. Reference POR and designed molecules POR1–POR5 optimized molecular geometries.

(E_g).^[36] The anti-bonding and bonding character of NFAs are clarified using LUMO and HOMO respectively. The ICT that reached to the end-capped acceptors from donor core determines the extent of voltage, current and cell effectiveness.^[37] The HOMO-LUMO E_g value is accountable for charge transformations among two molecular orbitals. If E_g will be lower, charge transformations will be high and vice versa. The results of individual molecular orbitals (HOMO, LUMO) energy and their energy gap results can be seen in Table 1.

The E_{HOMO} and E_{LUMO} of the reference POR were computed as -5.40 and -3.55 eV respectively with band gap value of 1.85 eV (Table 1). The E_{HOMO} s and E_{LUMO} s of the developed molecules POR1, POR2, POR3, POR4, POR5 was found to be -4.90 , -5.01 , -4.74 , -4.62 , -4.50 eV and -3.16 , -3.21 , -3.06 , -2.98 , -2.94 eV respectively (Table 1). These results show that proposed POR1–POR5 compounds occupy an attractive position in contrast to the reference POR. Besides the significance of LUMO, HOMO energies, energy gaps are also vital. The calculated E_g value of POR1 was computed as 1.73 eV which is 0.12 eV lesser when compared to the POR. The lowering in E_g value is due to P1 acceptor unit. The E_g value 1.80 eV in POR2 is found greater than POR1 but smaller than the reference POR molecule. This indicate the better efficiency of P2 acceptor than

the end-capped acceptor unit of POR. 0.17 eV reduction in E_g value is marked in the developed compound POR3 as compared to POR molecule due to incorporation of P3 end-capped acceptor unit. The E_g value decreases to 1.63 eV (0.22 eV lesser in comparison to the reference POR) due to better efficiency of P4. The lowest energy gap value 1.56 eV amongst all the studied compounds is found in the developed compound POR5. This might be because of the better electronegativity and extended conjugation of P5 used in POR5. Overall, E_g values order is found to be: $\text{POR5} < \text{POR4} < \text{POR3} < \text{POR1} < \text{POR2} < \text{POR}$. The lower values of E_g indicates an efficient designing of POR1–POR5 and their tendency to transmute greater charges, which will eventually help to expand the photovoltaic characteristics. Interestingly, all designed POR1–POR5 occupied a narrower E_g in contrast to the reference POR which makes them superior candidates for developing porphyrin-based NIR sensitive NFAs with remarkable optoelectronic properties.

FMO diagrams were further drawn and portrayed in Figure 5 to understand the charge transfer phenomenon. Studied molecules have demonstrated ability of charge transfer from D core to terminal A moieties via π -bridge. The π -bridge is accountable to provide better route for intramolecular charge transfer. In POR and POR1–POR5, HOMO is concentrated on the central porphyrin core. While, LUMO part is partially available on bridge 2-ethynyl-5-methylthiophene section and mainly on end-capped acceptors P1–P5 present in POR1–POR5 respectively. This transmission of charge from central D to end-capped after passing through bridge unit established a charge separation state which should ultimately boost the photovoltaic performances of these newly developed porphyrin-based NIR sensitive NFAs.

Molecules	HOMO (E_{HOMO})	LUMO (E_{LUMO})	$E_g = E_{\text{LUMO}} - E_{\text{HOMO}}$
POR	-5.40	-3.55	1.85
POR1	-4.90	-3.16	1.73
POR2	-5.01	-3.21	1.80
POR3	-4.74	-3.06	1.68
POR4	-4.62	-2.98	1.63
POR5	-4.50	-2.94	1.56

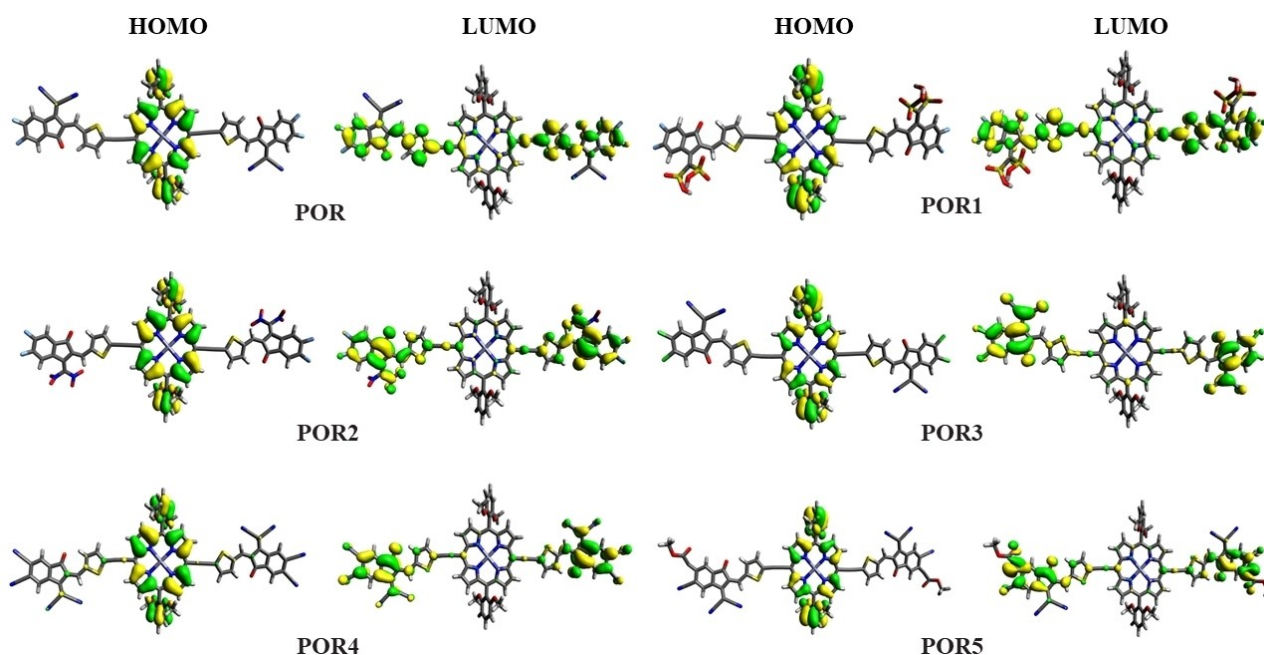


Figure 5. HOMOs and LUMOs of investigated molecules.

Density of state (DOS) and overlap population density of state analysis

The DOS and OPDOS analysis was completed for examining electronic distribution and absorption band in POR and POR1–POR5 and to support the FMOs analysis. DOS analysis are considered vital to estimate per unit increase in the energy levels. DOS values nearing zero indicate absence of the state, while large DOS values represents the accessibility of numerous states for a specific energy level. The DOS and OPDOS graphs portrayed in Figure 6 indicate that modified end-capped acceptor units had a significant impact on the distribution pattern around the HOMO and LUMO. To gain better understanding of the push-pull mechanisms of the ICT, investigated molecules POR and POR1–POR5 were separated into acceptor (A), bridge (B) and donor (D) fragments. These fragments are indicated with blue, green and red lines respectively on graphs indicated in Figure 6.

For HOMO of POR, donor, bridge and acceptor units contribute 60%, 29% and 11% respectively. Similarly, 8%, 17% and 75% is the contribution of donor, bridge and acceptor units towards LUMO of POR. In POR1, donor contributes 78% to HOMO and 4% LUMO, bridge contributes 12% to HOMO and 14% LUMO, whereas acceptor gives 10% to HOMO and 82% to LUMO. The donor moiety in POR2–POR5 contributes 62%, 74%, 61%, 84%, to HOMO and 7%, 14%, 5%, 6% to LUMO respectively. The percentage contribution of bridge unit to HOMO and LUMO of POR2–POR5 is 19%, 15%, 25%, 10% and 16%, 21%, 8%, 9% respectively. Similarly, acceptor segment contributes 17%, 11%, 14%, 6% to HOMO, whereas 77%, 65%, 87%, 85% to LUMO for POR2–POR5 respectively.

All findings indicate that HOMO density in POR1–POR5 is concentrated on the central core donor, whereas, LUMO is populated on terminal acceptor portion and slight on bridge unit. The charge density transfers from donor to bridge and then to the end-capped acceptors represent the successful intramolecular charge transfer. This is a confirmation of our effective end-capped alterations strategy to develop new and efficient porphyrin-based near-infrared sensitive NFAs with promising photovoltaic characteristics for OSCs applications.

Optical Properties

The optimal design of efficient photovoltaic molecules is grounded in their favorable optical properties.^[38] Therefore, these were investigated for POR and POR1–POR5 are with TDDFT calculations and results of calculated optical characteristics (E_{sv} , λ_{max} , f_{os} and transition natures) of POR and POR1–POR5 given in Table 2. The absorption spectrum of POR and POR1–POR5 is pictographically portrayed in Figure 7.

The TDDFT results showed that the computed value of 840 nm of POR was found practically close to the experimental absorption (λ_{max}) value of 810 nm of POR. Structural tailoring of reference POR molecule with P1 end-capped acceptor unit significantly altered the optical properties and gave the value of 906 nm λ_{max} value for POR1, which is 66 nm red-shifted from

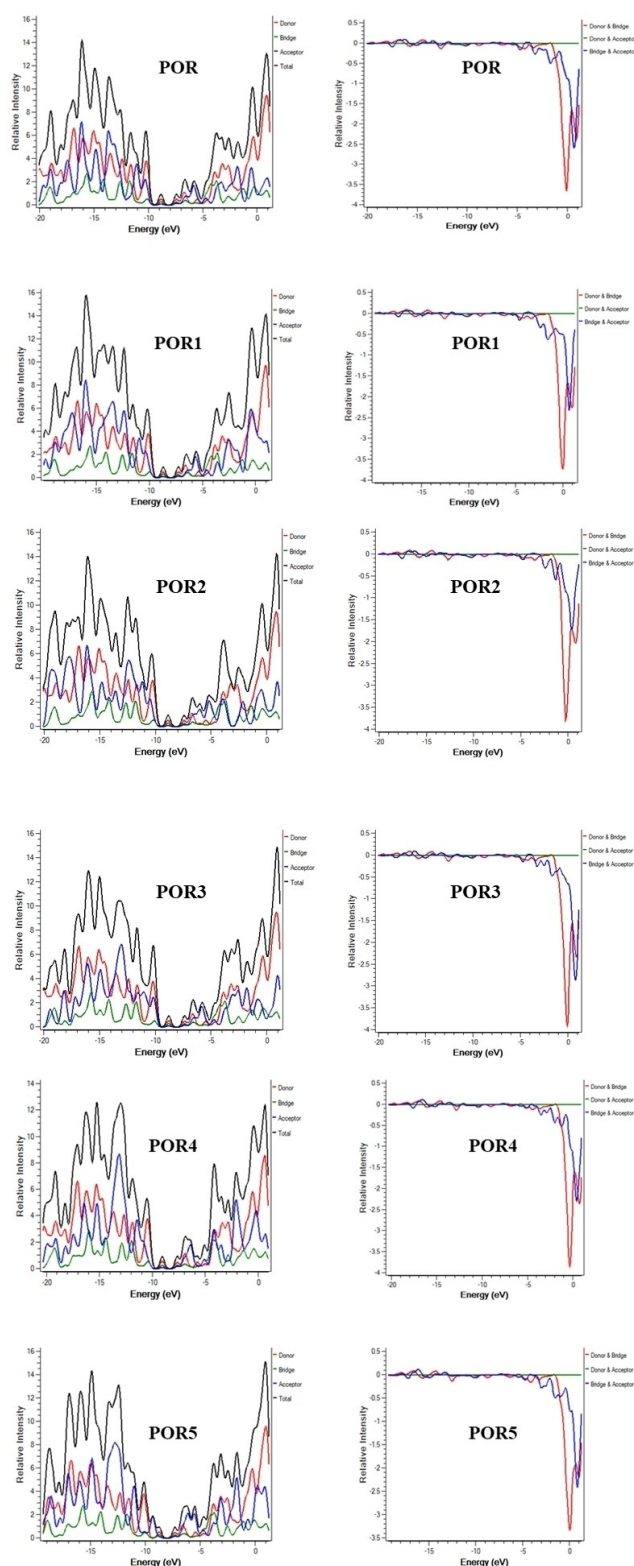


Figure 6. The DOS and OPDOS plots of POR and POR1–POR5.

POR (Table 2 and Figure 7). The λ_{max} of POR2 is also red-shifted to 898.82 nm. This implies that P2 end-capped unit performance for tuning the λ_{max} value is found greater than reference POR but minutely smaller than P1 end-capped unit used in POR1.

Molecule	E_x [eV]	λ_{max} [nm]	f	Major electron transportation [%]
POR	1.47	840.05 (810) ^a	2.72	HOMO→LUMO (89%)
POR1	1.35	906.50	3.45	HOMO→LUMO (93%)
POR2	1.37	898.82	3.03	HOMO→LUMO (86%)
POR3	1.35	907.45	3.31	HOMO→LUMO (89%)
POR4	1.37	913.54	1.09	HOMO→LUMO (87%)
POR5	1.11	1116.27	1.21	HOMO→LUMO (97%)

[a] Exp. value in parentheses is from the reference.^[17]

The efficiency of P3 end-capped acceptor was found to be marginally better in red shifting the λ_{max} value of POR3 to 907.45 nm than reference molecule. End-capped modification in POR4 made augmented the optical properties and shifted the λ_{max} value to 913.54 nm. End-capped substitution is considered as a very good approach in designing novel NFAs and has definitely proven itself in POR5 where highest red-shift in λ_{max} value to 1116.27 nm is noted among all studied compounds (Table 2 and Figure 7). The extension in λ_{max} values as compared to reference molecule indicate that all designed POR1–POR5 molecules occupied near-infrared (NIR) sensitive absorption region. Currently, expansion of NIR spectrum utilized light-harvesting systems have extensive importance. In organic photovoltaics, the active layer's absorption spectral range is broadened by introducing NIR photoelectric materials, which results in the adequate handling of the solar spectrum for efficiently augmenting the photon-harvesting ability. The

photoelectric conversion efficiency and the short-circuit current of the devices are promoted using NIR materials introduction strategy.^[39] These NIR materials based photovoltaic devices own the numerous aspects of heat insulation, power generation, light transmission, which can be used in self-powered greenhouses, automobiles, and on facades of buildings.^[40] The NIR absorbing features of investigated compounds indicate that they have a great potential to become excellent photovoltaic materials for manufacturing solar cells devices.

Excitation energy (E_x) is another vital factor which evaluates the photovoltaic efficiency of NFAs. Usually, good efficiency in solar cell is exhibited by the molecules containing low excitation energy. The calculated E_x parameters of the reference and developed POR1–POR5 NFAs were found to be 1.47 eV and 1.35, 1.37, 1.35, 1.37, 1.11 eV respectively. It's quite fascinating that all the modified compounds demonstrated lower excitation energy in contrast to the POR thus endorsing the effective potential for developing porphyrin-based near-infrared sensitive NFAs.

Open circuit voltage

To estimate the OSCs effectiveness, competency of the device and to govern the entire current drained from the device, V_{oc} is employed.^[29] In other words, maximum voltage provided by the solar cell is represented in term of V_{oc} . Recombination amount in OSCs is measured with the assistance of V_{oc} . Scharber's equation^[41] utilization of the HOMO of donor and LUMO of acceptor for the measurement of V_{oc} is determined as follows:

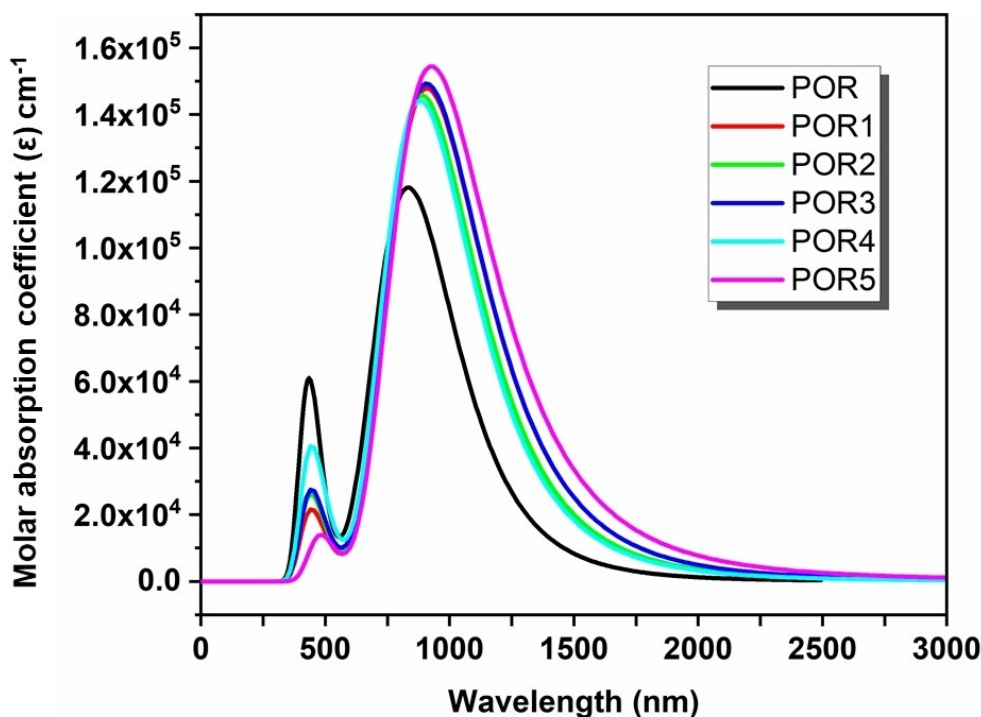


Figure 7. The UV-Visible absorption spectra of POR and POR1–POR5.

$$V_{oc} = (|E_{HOMO}^D| - |E_{LUMO}^A|) - 0.3 \quad (3)$$

Since the investigated molecules POR and POR1–POR5 are the acceptors, therefore, established PTB7-Th polymer is used as donor to make blend with the developed acceptor molecules. The V_{oc} results obtained from Scharber's equation 3 in accordance with $HOMO_{PTB7-Th} - LUMO_{Acceptor}$ energy gaps are represented in Table 3.

It is clear from Table 3 that V_{oc} for reference POR molecule is found to be 1.35 V. Due to lower energy gap, better absorption maximum values and lower transition energy values in all designed molecules than the reference POR, the V_{oc} of all modified compounds is found superior than the reference POR. The V_{oc} for the newly developed POR1–POR5 are computed 1.74, 1.69, 1.84, 1.92 and 1.96 V respectively. The highest open circuit voltage value is exhibited by POR5. The decreasing order of V_{oc} for entitled NFAs is found to be $POR5 > POR4 > POR3 > POR1 > POR2 > POR$. This order matches well with their above mentioned electronic and optical properties. It is generally considered that for achieving high conversion efficiency, high V_{oc} results are known to be important. Higher V_{oc} values represent the larger voltage obtained from solar cell, high conversion efficiency and vice versa. All developed molecules POR1–POR5 of studied family with greater than reference V_{oc} values can be considered as better entrants for achieving maximum voltage from solar cell and high conversion efficiency as compared to POR.

Reorganization energy

The organic solar cells performance and charge mobilities are estimated using hole and electron reorganization energies to evaluate the necessary relationship between the structure of molecules and the charge transportation. Charge mobilities are inversely related to the reorganization energy, thus, lower

Table 3. V_{oc} of studied acceptor molecules with respect to PTB7-Th donor polymer.			
Molecule	E_{HOMO}^D	E_{LUMO}^A	V_{oc}
POR	−5.20	−3.55	1.35
POR1	−5.20	−3.16	1.74
POR2	−5.20	−3.21	1.69
POR3	−5.20	−3.06	1.84
POR4	−5.20	−2.98	1.92
POR5	−5.20	−2.94	1.96

Table 4. Reorganization energy (in E_h) of electron and hole for POR and POR1–POR5.		
Molecules	λ_e [Eh]	λ_h [Eh]
POR	0.007939	0.006674
POR 1	0.007702	0.006412
POR 2	0.007821	0.006507
POR 3	0.007678	0.006090
POR 4	0.007261	0.005992
POR 5	0.007013	0.004686

reorganization energy values result in higher charge mobilities and vice versa. The calculated reorganization energy values with respect to equations 1 and 2 are given in Table 4.

The λ_e and λ_h values of reference POR molecule are computed as $0.007939 E_h$ and $0.006674 E_h$ respectively. End-capped acceptor P1 in POR1 lowers the λ_e and λ_h values to 0.007702 and $0.006412 E_h$ respectively. Similarly, P2 end-capped acceptor successfully lowers the λ_e and λ_h values in POR2 as compared to reference POR but these values are slightly greater in contrast to POR1 indicating the better hole and electron mobilities than the reference but less than POR1. Further reduction in λ_e and λ_h values of compounds POR3, POR4 and POR5 are noted as compared to the reference POR, exhibiting the effectiveness of P3, P4 and P5 end-capped acceptors. Interestingly, all designed molecules were found with lower λ_e and λ_h values than the reference POR, where POR5 had the lowest λ_e and λ_h values with $0.007013 E_h$ and $0.004686 E_h$. The trend of λ_e and λ_h values among all of the newly developed porphyrin-based NFAs (POR1–POR5) is: $POR5 < POR4 < POR3 < POR1 < POR2 < POR$ and $POR5 < POR4 < POR3 < POR1 < POR2 < POR$ correspondingly. It is evident from this order that the newly proposed molecules have great potential to become efficient hole and electron transport materials in solar cells devices.

Transition density matrix (TDMs) analysis

To comprehend the diverse excited state charge transitions especially from ground (S_0) to an excited (S_1) state present in investigated molecules, TDMs investigation was performed.^[33] The transitions of charge on each atom is represented in the heat map as vertical band of colors (Figure 8). The charge density, hole-electron coupling and position of electrons and holes are also elucidated from TDM analysis and indicated in Figure 9. The number of atoms of each investigated molecule except hydrogen which is neglected due to little contribution can be seen on the vertical and horizontal axis.

The TDM map shows the coherence of electrons. The POR and developed POR1–POR4 molecules are very similar in terms of charge distribution with strong charge density on central donor unit porphyrin ring. The transitions of charge initiate from atoms 1–21 of the porphyrin ring. The charge shifts to atoms 25–37, which is the bridge portion of the reference and designed molecules. Following on the atom numbers > 51 are the acceptor unit attracting the charge density creating an intramolecular charge separation state. The behavior of POR5 molecule is different as compared to other designed molecules, where a diagonal charge transfer is observed and significant charge density is found on the end-capped acceptor. This indicates the effectiveness of end-capped acceptor P5 used in POR5 in withdrawing the charge density from the central core to itself. It can be seen in all the molecules that when central core porphyrin unit is augmented with the end-capped acceptors P1–P5, charge density flow lingers successfully inside the entire molecule. These TDM studies show that developed

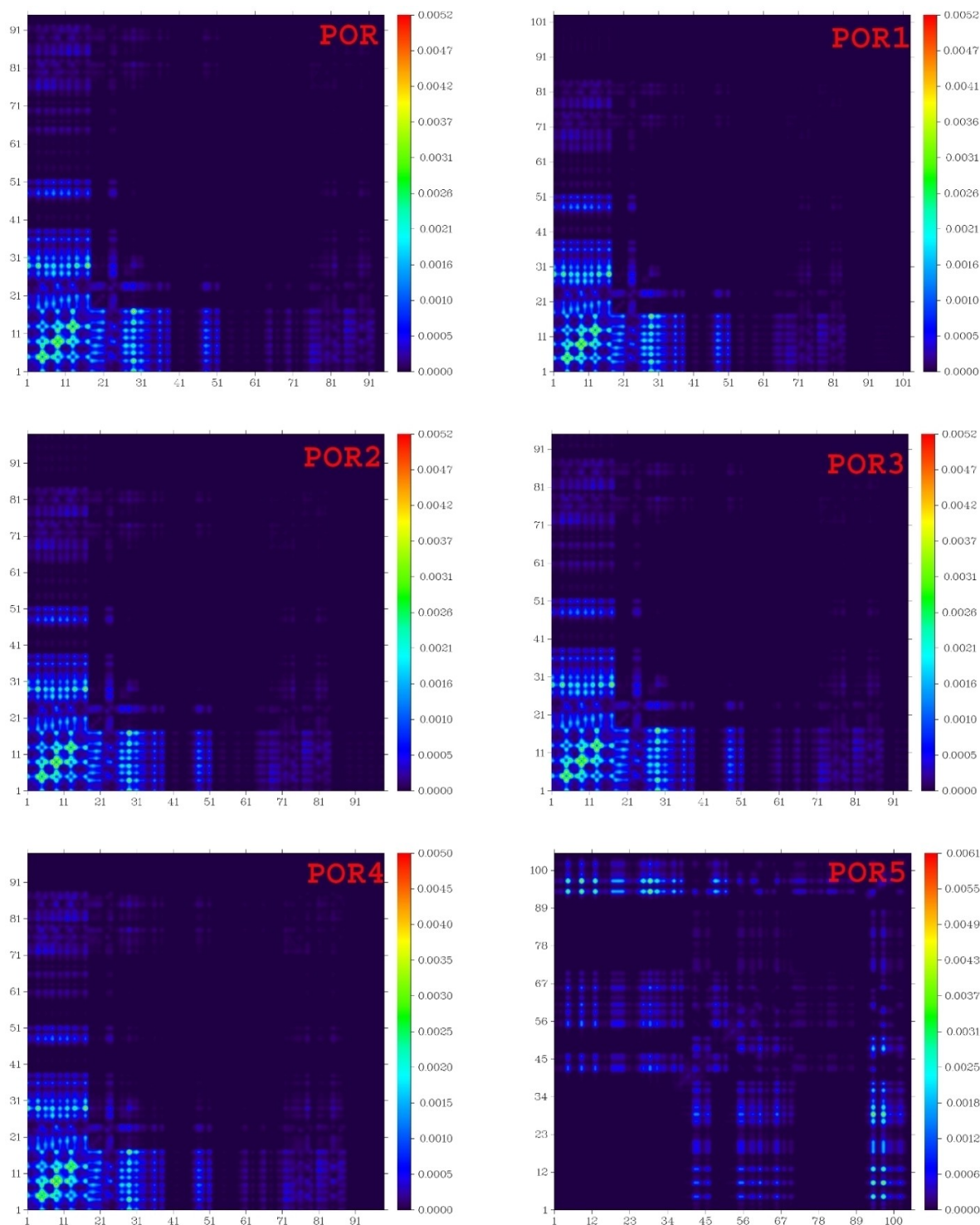


Figure 8. Transition density matrix of POR and POR1–POR5 from ground (S_0) to an excited (S_1) state.

molecules especially POR5 could be a superior contender as an acceptor material for OSCs applications.

Exciton binding Energy (E_b)

Binding energy is also considered as a promising aspect for estimating the optoelectronic assets of OSCs which aids in the explanation of exciton dissociation capacity.^[42] The E_b analysis is used to measure the hole-electron Coulombic interaction, where high interactions are found in molecules with low E_b

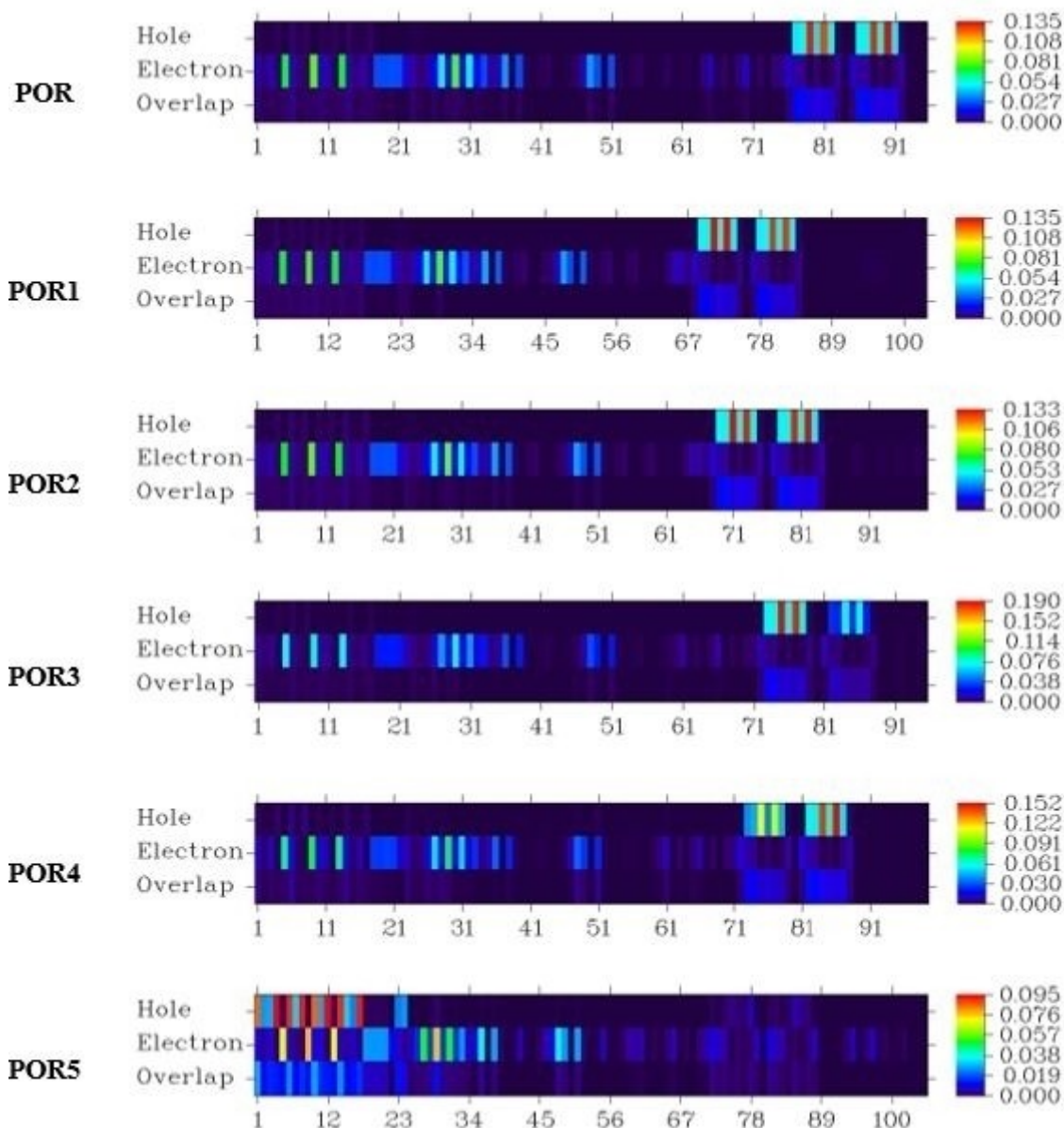


Figure 9. Electron-hole overlap transition density matrix of all studied molecules in excited state.

values, resulting in higher current density and thus enhancing PCE of OSCs devices. Equation 4 is utilized to calculate the E_b which is the difference of energy gap and first singlet vertical excitation energy obtained from TDDFT calculations, the results are mentioned in the Table 5.

Molecules	E_{H-L} [eV]	$E_{vertical}$ [eV]	E_b [eV]
POR	1.85	0.617	1.232
POR1	1.73	0.575	1.154
POR2	1.80	0.570	1.229
POR3	1.68	0.562	1.117
POR4	1.63	0.596	1.033
POR5	1.56	0.573	0.986

$$E_b = E_{H-L} - E_{vertical} \quad (4)$$

The E_b of reference POR molecule is noted as 1.232 eV. In designed molecule POR1, the E_b value is found to be higher than the reference molecule indicating the lower hole-electron coupling as shown in Figure 10. All modified compounds except POR1 exhibit lower E_b values than POR indicating the strong hole and electron coulombic interaction. These values are 1.229, 1.117, 1.033 and 0.986 eV in POR2, POR3, POR4 and POR5 respectively. The lowest binding energy value is computed for POR5 which makes it comparatively the most efficient. The order of E_b is reported as POR5 < POR4 < POR3 < POR2 < POR < POR1 which shows the effectiveness of the proposed end-capped acceptor units.

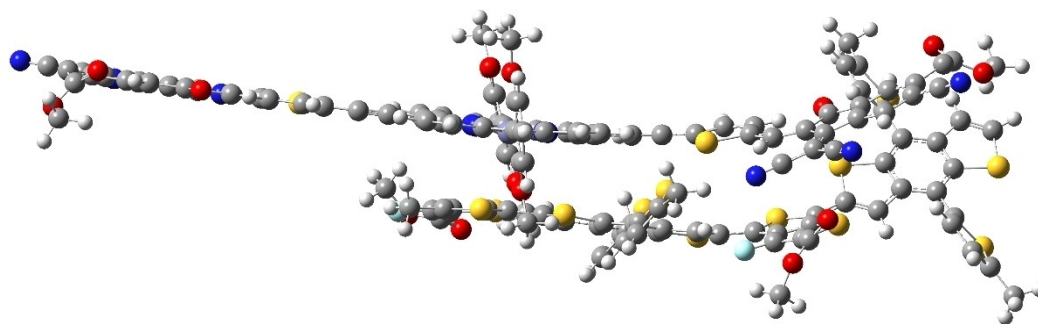


Figure 10. Optimized geometry of PTB7-Th:POR5 blend.

Charge transfer analysis of acceptor POR5 and polymer PTB7-Th as the donor

Charge transfer analysis is used to confirm the applicability of the designed molecules in bulk heterojunction materials, they are modelled into a layer with a known and well characterized donor. POR5 molecule owing to its lowest E_{H-L} , lowest E_x , lowest E_{br} , lowest λ_e and λ_{hr} , NIR λ_{max} , and highest V_{oc} values among all investigated systems was selected for charge transfer analysis with established PTB7-Th^[43] polymer is made and PTB7-Th:POR5 complex has been optimized. The PTB7-Th:POR5 complex optimized geometry is given in Figure 10. The position of PTB7-Th is below and POR5 is at top in the Figure 10. For electron transfer procedure, the orientation of PTB7-Th:POR5 complex is also supportive. The parallel orientation of central parts of POR5 and PTB7-Th promotes the transfer of charge among donor and acceptor moieties.

The FMO analysis of PTB7-Th:POR5 complex indicated that HOMO charge density in PTB7-Th:POR5 blend is present on donor PTB7-Th polymer (Figure 11). While, LUMO portion in PTB7-Th:POR5 complex is found on acceptor POR5 molecule. The transmission of charge density from donor to acceptor layer in PTB7-Th:POR5 blend is a strong indication for utility of designed molecules in practical solar cell applications.

Conclusion

An interactive design computation of porphyrin-based NIR sensitive NFAs has been proposed herein to be used in highly efficient panchromatic organic solar cells applications. Results conclude that abridged energy gap in span of 1.80–1.56 eV is found in proposed compounds when compared with the reference's POR of 1.86 eV. This is due to the extended

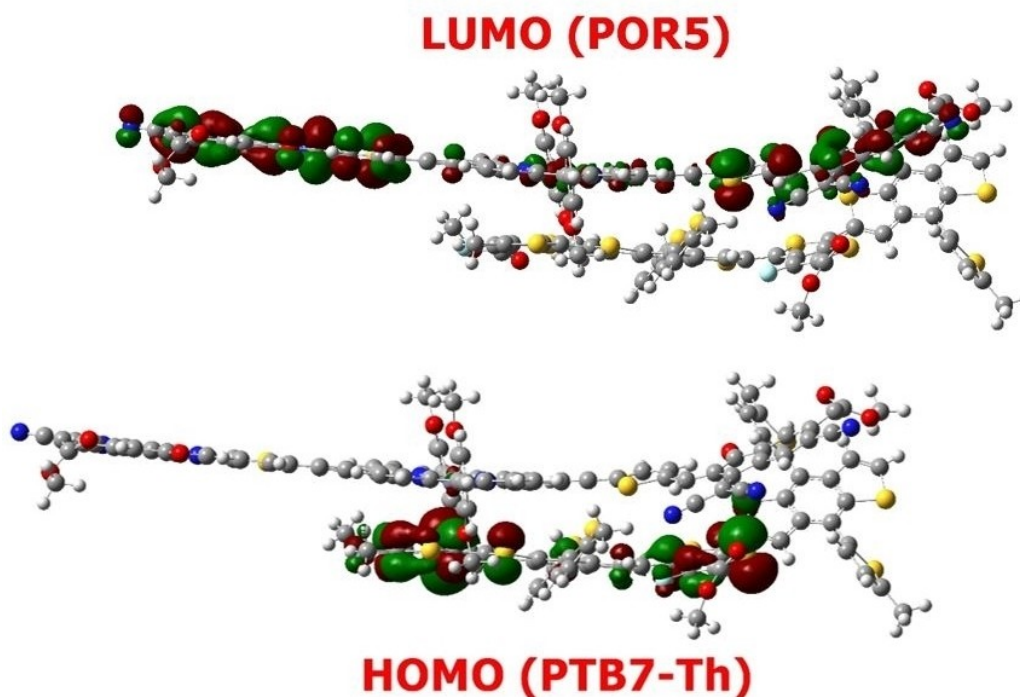


Figure 11. HOMO and LUMO distribution patterns on PTB7-Th and POR5 of PTB7-Th:POR5 complex respectively.

conjugation and better electron withdrawing capability of end-capped acceptors P1-P5 used in the proposed POR1–POR5 molecule. DOS analysis confirms that donor moiety in POR1–POR5 contributes 78%, 62%, 74%, 61%, 84%, to HOMO and 4%, 7%, 14%, 5%, 6% to LUMO respectively. While acceptor segment contributes 10%, 17%, 11%, 14%, 6% to HOMO, whereas 82%, 77%, 65%, 87%, 85% to LUMO for POR1–POR5 respectively. Structural tailoring of reference POR with P1-P5 end-capped acceptor units significantly tune the λ_{max} values which are found red-shifted and in near infrared region 898.82–1116.27 nm in POR1–POR5 as compared to reference POR 840.05 nm. All proposed molecules also exhibit lower excitation energy values 1.37–1.11 eV than POR's 1.47 eV with 86–93% electron transportation from HOMO→LUMO. Maximum current with respect to HOMO_{PTB7-Th}-LUMO_{Acceptor} can be withdrawn from proposed molecules is proven from open-circuit voltage results which are found to be V_{oc} = 1.74, 1.69, 1.84, 1.92, 1.96 V for POR1–POR5 respectively and better in contrast to the reference's V_{oc} at 1.35 V. The λ_e and λ_h values successfully lower from 0.007939 E_h and 0.006674 E_h respectively in reference POR to 0.007821–0.007013 E_h and 0.006507–0.004686 E_h in proposed molecule POR1–POR5 respectively. TDM analysis confirm that coherence of charge density in reference POR and developed POR1–POR4 molecules is almost similar with strong charge density on central donor unit porphyrin ring. Charge transfer analysis proved the charge transfer from HOMO_{PTB7-Th} to LUMO_{POR5} in PTB7-Th:POR5 blend. All proposed compounds except POR1 exhibit lower binding energy values than POR indicating the strong hole and electron coulombic interaction. The energy gap, excitation energy, λ_e , λ_h values are observed in order of: POR5 < POR4 < POR3 < POR1 < POR2 < POR which is exactly inverse to λ_{max} and V_{oc} decreasing order: POR5 > POR4 > POR3 > POR1 > POR2 > POR. As a whole, the designed molecules POR1–POR5 especially POR5 exhibit superior optoelectronic properties than reference POR. Thus, proposed porphyrin-based NIR sensitive NFA derivatives are recommended to be used in panchromatic organic solar cells applications.

Acknowledgment

Funding in the Lu lab was provided by the Fundamental Research Funds for the Central Universities (2232021G-04), Shanghai Science and Technology Committee (19ZR1471100). M. A. A and M. I. appreciates the support of the Research Center for Advanced Materials Science at King Khalid University Saudi Arabia through research groups program under grant number KKU/RCAMS/22.

Conflict of Interest

The authors declare no conflict of interest.

Data Availability Statement

The data that support the findings of this study are available from the corresponding author upon reasonable request.

Keywords: DFT · Near-infrared sensitive · Non-fullerene Acceptors · Organic solar cells · Porphyrins;

- [1] T. R. Cook, D. K. Dogutan, S. Y. Reece, Y. Surendranath, T. S. Teets, D. G. Nocera, *Chem. Rev.* **2010**, *110*, 6474–6502.
- [2] V. S. Arutyunov, G. V. Lisichkin, *Russ. Chem. Rev.* **2017**, *86*, 777.
- [3] D. J. Des Marais, *Science* **2000**, *289*, 1703–1705.
- [4] A. A. Ryan, M. O. Senge, *Photochem. Photobiol. Sci.* **2015**, *14*, 638–660.
- [5] a) L. Bucher, N. Desbois, P. D. Harvey, G. D. Sharma, C. P. Gros, *Solar RRL* **2017**, *1*, 1700127; b) A. Mahmood, J.-Y. Hu, B. Xiao, A. Tang, X. Wang, E. Zhou, *J. Mater. Chem. A* **2018**, *6*, 16769–16797; c) G. Di Carlo, A. Orbelli Biroli, M. Pizzotti, F. Tessoro, *Front. Chem.* **2019**, *7*, 177; d) J. Lu, S. Liu, M. Wang, *Front. Chem.* **2018**, *6*, 541.
- [6] a) V. Cuesta, M. Vartanian, P. de la Cruz, R. Singhal, G. D. Sharma, F. Langa, *J. Mater. Chem. A* **2017**, *5*, 1057–1065; b) S. Chen, L. Yan, L. Xiao, K. Gao, W. Tang, C. Wang, C. Zhu, X. Wang, F. Liu, X. Peng, *J. Mater. Chem. A* **2017**, *5*, 25460–25468; c) G. Yang, Y. Tang, X. Li, H. Ågren, Y. Xie, *ACS Appl. Mater. Interfaces* **2017**, *9*, 36875–36885.
- [7] a) X. Huang, C. Zhu, S. Zhang, W. Li, Y. Guo, X. Zhan, Y. Liu, Z. Bo, *Macromolecules* **2008**, *41*, 6895–6902; b) T. Umeyama, T. Takamatsu, N. Tezuka, Y. Matano, Y. Araki, T. Wada, O. Yoshikawa, T. Sagawa, S. Yoshikawa, H. Imahori, *J. Phys. Chem. C* **2009**, *113*, 10798–10806; c) N. Xiang, Y. Liu, W. Zhou, H. Huang, X. Guo, Z. Tan, B. Zhao, P. Shen, S. Tan, *Eur. Polym. J.* **2010**, *46*, 1084–1092; d) J. Y. Lee, H. J. Song, S. M. Lee, J. H. Lee, D. K. Moon, *Eur. Polym. J.* **2011**, *47*, 1686–1693.
- [8] a) W. Zhou, P. Shen, B. Zhao, P. Jiang, L. Deng, S. Tan, *J. Polym. Sci. Part A* **2011**, *49*, 2685–2692; b) H. Zhan, S. Lamare, A. Ng, T. Kenny, H. Guernon, W.-K. Chan, A. B. Djurišić, P. D. Harvey, W.-Y. Wong, *Macromolecules* **2011**, *44*, 5155–5167; c) S. Shi, P. Jiang, S. Chen, Y. Sun, X. Wang, K. Wang, S. Shen, X. Li, Y. Li, H. Wang, *Macromolecules* **2012**, *45*, 7806–7814; d) L. Wang, Z. Qiao, C. Gao, J. Liu, Z.-G. Zhang, X. Li, Y. Li, H. Wang, *Macromolecules* **2016**, *49*, 3723–3732.
- [9] Y. H. Chao, J. F. Jheng, J. S. Wu, K. Y. Wu, H. H. Peng, M. C. Tsai, C. L. Wang, Y. N. Hsiao, C. L. Wang, C. Y. Lin, *Adv. Mater.* **2014**, *26*, 5205–5210.
- [10] a) T. Liang, L. Xiao, K. Gao, W. Xu, X. Peng, Y. Cao, *ACS Appl. Mater. Interfaces* **2017**, *9*, 7131–7138; b) T. Lai, X. Chen, L. Xiao, L. Zhang, T. Liang, X. Peng, Y. Cao, *Chem. Commun.* **2017**, *53*, 5113–5116; c) L. Xiao, S. Chen, X. Chen, X. Peng, Y. Cao, X. Zhu, *J. Mater. Chem. C* **2018**, *6*, 3341–3345; d) L. Xiao, T. Lai, X. Liu, F. Liu, T. P. Russell, Y. Liu, F. Huang, X. Peng, Y. Cao, *J. Mater. Chem. A* **2018**, *6*, 18469–18478.
- [11] W. T. Hadmojo, U.-H. Lee, D. Yim, H. W. Kim, W.-D. Jang, S. C. Yoon, I. H. Jung, S.-Y. Jang, *ACS Appl. Mater. Interfaces* **2018**, *10*, 41344–41349.
- [12] A. Zhang, C. Li, F. Yang, J. Zhang, Z. Wang, Z. Wei, W. Li, *Angew. Chem. Int. Ed.* **2017**, *56*, 2694–2698; *Angew. Chem.* **2017**, *129*, 2738–2742.
- [13] a) Z.-Q. Jiang, T.-T. Wang, F.-P. Wu, J.-D. Lin, L.-S. Liao, *J. Mater. Chem. A* **2018**, *6*, 17256–17287; b) D. He, F. Zhao, L. Jiang, C. Wang, *J. Mater. Chem. A* **2018**, *6*, 8839–8854.
- [14] J. Mai, Y. Xiao, G. Zhou, J. Wang, J. Zhu, N. Zhao, X. Zhan, X. Lu, *Adv. Mater.* **2018**, *30*, 1802888.
- [15] L. Zhu, M. Zhang, G. Zhou, T. Hao, J. Xu, J. Wang, C. Qiu, N. Prine, J. Ali, W. Feng, *Adv. Energy Mater.* **2020**, *10*, 1904234.
- [16] M.-C. Tsai, C.-M. Hung, Z.-Q. Chen, Y.-C. Chiu, H.-C. Chen, C.-Y. Lin, *ACS Appl. Mater. Interfaces* **2019**, *11*, 45991–45998.
- [17] W.-C. Wang, Y.-W. Lin, S.-H. Peng, C.-T. Chuang, C.-C. Chang, C.-S. Hsu, *Org. Electron.* **2020**, *86*, 105899.
- [18] M. J. Frisch, G. W. Trucks, H. B. Schlegel, G. Scuseria, M. A. Robb, J. R. Cheeseman, G. Scalmani, V. Barone, B. Mennucci, G. Petersson, H. Nakatsuji, M. Caricato, X. Li, H. P. Hratchian, A. F. Izmaylov, J. Bloino, G. Zheng, J. L. Sonnenberg, M. Hada, M. Ehara, K. Toyota, R. Fukuda, J. Hasegawa, M. Ishida, T. Nakajima, Y. Honda, O. Kitao, H. Nakai, T. Vreven, J. A. Montgomery, J. E. Peralta, F. Ogliaro, M. Bearpark, J. J. Heyd, E. Brothers, K. N. Kudin, V. N. Staroverov, R. Kobayashi, J. Normand, K. Raghavachari, A. Rendell, J. C. Burant, S. S. Iyengar, J. Tomasi, M. Cossi, N. Rega, J. M. Millam, M. Klene, J. E. Knox, J. B. Cross, V. Bakken, C. Adamo, J. Jaramillo, R. Gomperts, R. E. Stratmann, O. Yazyev, A. J. Austin, R. Cammi, C. Pomelli, J. W. Ochterski, R. L. Martin, K. Morokuma, V. J.

- Zakrzewski, G. A. Voth, P. Salvador, J. J. Dannenberg, S. Dapprich, A. D. Daniels, O. Farkas, J. B. Foresman, J. V. Ortiz, J. Cioslowski, D. 0109, Gaussian Inc., Wallingford, CT 2009.
- [19] R. D. Dennington, T. A. Keith, J. M. Millam, *Gaussian Inc* 2008.
- [20] a) M. Khalid, M. Imran, A. A. C. Braga, M. S. Akram, *Sci. Rep.* 2021, 11, 20320; b) M. U. Khan, R. Hussain, M. Y. Mehboob, M. Khalid, M. A. Ehsan, A. Rehman, M. R. S. A. Janjua, *Spectrochim. Acta. A Mol. Biomol. Spectrosc.* 2021, 245, 118938; c) M. U. Khan, R. Hussain, M. Yasir Mehboob, M. Khalid, Z. Shafiq, M. Aslam, A. A. Al-Saadi, S. Jamil, M. R. S. A. Janjua, *ACS Omega* 2020, 5, 24125–24137; d) A. Rafiq, R. Hussain, M. U. Khan, M. Y. Mehboob, M. Khalid, M. M. Alam, M. Imran, K. Ayub, *Energy Technol.* 2022, 10 (3), 2100751.
- [21] B. Civalleri, C. M. Zicovich-Wilson, L. Valenzano, P. Ugliengo, *CrystEng-Comm* 2008, 10, 405–410.
- [22] J.-D. Chai, M. Head-Gordon, *Phys. Chem. Chem. Phys.* 2008, 10, 6615–6620.
- [23] C. Adamo, V. Barone, *J. Chem. Phys.* 1998, 108, 664–675.
- [24] H. Iikura, T. Tsuneda, T. Yanai, K. Hirao, *J. Chem. Phys.* 2001, 115, 3540–3544.
- [25] T. Yanai, D. P. Tew, N. C. Handy, *Chem. Phys. Lett.* 2004, 393, 51–57.
- [26] Y. Zhao, D. G. Truhlar, *Theor. Chem. Acc.* 2008, 120, 215–241.
- [27] V. Barone, M. Cossi, *J. Phys. Chem. A* 1998, 102, 1995–2001.
- [28] a) M. U. Khan, J. Iqbal, M. Khalid, R. Hussain, A. A. C. Braga, M. Hussain, S. Muhammad, *RSC Adv.* 2019, 9, 26402–26418; b) M. U. Khan, M. Khalid, M. N. Arshad, M. N. Khan, M. Usman, A. Ali, B. Saifullah, *ACS Omega* 2020, 5, 23039–23052.
- [29] S. Tang, J. Zhang, *J. Comput. Chem.* 2012, 33, 1353–1363.
- [30] N. M. O'boyle, A. L. Tenderholt, K. M. Langner, *J. Comput. Chem.* 2008, 29, 839–845.
- [31] M. D. Hanwell, D. E. Curtis, D. C. Lonie, T. Vandermeersch, E. Zurek, G. R. Hutchison, *J. Cheminf.* 2012, 4, 17.
- [32] G. A. Andrienko, Chemcraft – graphical software for visualization of quantum chemistry computations. <https://www.chemcraftprog.com>, 2010.
- [33] T. Lu, F. Chen, *J. Comput. Chem.* 2012, 33, 580–592.
- [34] a) M. Khalid, M. U. Khan, S. Ahmed, Z. Shafiq, M. M. Alam, M. Imran, A. A. C. Braga, M. S. Akram, *Sci. Rep.* 2021, 11, 1–15; b) M. Khalid, M. U. Khan, E. t. -Razia, Z. Shafiq, M. M. Alam, M. Imran, M. S. Akram, *Sci. Rep.* 2021, 11, 19931.
- [35] A. Mahmood, *J. Cluster Sci.* 2019, 30, 1123–1130.
- [36] M. U. Khan, M. Khalid, R. Hussain, A. Umar, M. Y. Mehboob, Z. Shafiq, M. Imran, A. Irfan, *Energy Fuels* 2021, 35, 12436–12450.
- [37] a) M. U. Khan, M. Khalid, M. Ibrahim, A. A. C. Braga, M. Safdar, A. A. Al-Saadi, M. R. S. A. Janjua, *J. Phys. Chem. C* 2018, 122, 4009–4018; b) M. R. S. A. Janjua, M. U. Khan, B. Bashir, M. A. Iqbal, Y. Song, S. A. R. Naqvi, Z. A. Khan, *Comp. Theor. Chem.* 2012, 994, 34–40; c) M. R. S. A. Janjua, M. Amin, M. Ali, B. Bashir, M. U. Khan, M. A. Iqbal, W. Guan, L. Yan, Z. M. Su, *Eur. J. Inorg. Chem.* 2012, 2012, 705–711; d) M. U. Khan, M. Ibrahim, M. Khalid, M. S. Qureshi, T. Gulzar, K. M. Zia, A. A. Al-Saadi, M. R. S. A. Janjua, *Chem. Phys. Lett.* 2019, 715, 222–230; e) M. U. Khan, M. Ibrahim, M. Khalid, A. A. C. Braga, S. Ahmed, A. Sultan, *J. Cluster Sci.* 2019, 30, 415–430; f) M. U. Khan, M. Ibrahim, M. Khalid, S. Jamil, A. A. Al-Saadi, M. R. S. A. Janjua, *Chem. Phys. Lett.* 2019, 719, 59–66; g) M. R. S. A. Janjua, M. U. Khan, M. Khalid, N. Ullah, R. Kalgaonkar, K. Alnoaimi, N. Baqader, S. Jamil, *J. Cluster Sci.* 2021, 32 (2), 243–253.
- [38] M. Khalid, I. Shafiq, M. Zhu, M. U. Khan, Z. Shafiq, J. Iqbal, M. M. Alam, A. A. C. Braga, M. Imran, *J. Saudi Chem. Soc.* 2021, 25, 101305.
- [39] B. Xie, Z. Chen, L. Ying, F. Huang, Y. Cao, *InfoMat* 2020, 2, 57–91.
- [40] C. Sun, R. Xia, H. Shi, H. Yao, X. Liu, J. Hou, F. Huang, H.-L. Yip, Y. Cao, *Joule* 2018, 2, 1816–1826.
- [41] M. C. Scharber, D. Mühlbacher, M. Koppe, P. Denk, C. Waldauf, A. J. Heeger, C. J. Brabec, *Adv. Mater.* 2006, 18, 789–794.
- [42] Y. Zhu, F. Zhao, W. Wang, Y. Li, S. Zhang, Y. Lin, *Adv. Energy and Sustainability Res.* 2022, 3, 2100184.
- [43] B. Xiao, Y. Zhao, A. Tang, H. Wang, J. Yang, E. Zhou, *Sci. Bull.* 2017, 62, 1275–1282.

Manuscript received: March 6, 2022

Revised manuscript received: July 6, 2022